Electronic Supplementary Material (ESI) for Physical Chemistry Chemical Physics

High-Resolution Solid-State ^{13}C NMR Spectroscopy of the Paramagnetic Metal-Organic Frameworks, STAM-1 and HKUST-1

Supporting Information

Daniel M. Dawson, Lauren E. Jamieson, M. Infas H. Mohideen, Alistair C. McKinlay, Iain A. Smellie, Romain Cadou, Neil S. Keddie, Russell E. Morris and Sharon E. Ashbrook

S1. Synthesis and characterisation of ^{13}C-labelled organic linkers

S2. Synthesis of Cu-based MOFs

S3. Packing of moisture-sensitive samples into NMR rotors

S4. Inversion recovery measurement of T_1

S5. Solution-state and solid-state NMR spectra for tmbtc and H_3btc

S6. Isotropic shifts, T_1 and linewidths for ^{13}C resonances of as-made STAM-1 (14.1 T)

S7. ^{1}H NMR of CD_3-STAM-1

S8. X-ray diffraction patterns of isotopically-enriched ^{13}C(1,3,4,5)-STAM-1

S9. Extraction of isotopically-enriched mmbtc

S10. ^{13}C NMR spectra of dehydrated ^{13}C(2,6)-STAM-1

S11. ^{13}C shifts and T_1 relaxation constants at 9.4, 14.1 and 20.0 T

S12. References

S1. Synthesis and characterisation of ^{13}C-labelled organic linkers

1[^{13}C],3,5-Trimethylbenzene

A mixture of 3,5-dimethylbromobenzene (6.84 g, 37 mmol) and THF (80 ml) was cooled to –78 °C before *n*-BuLi (2.5 M in hexane, 14.8 mL) was added. The resulting aryl lithium solution was stirred for 1 h before [^{13}C]iodomethane (5.00 g; 35 mmol) was added. The mixture was stirred for 2 h and then warmed to room temperature. THF and any unreacted [^{13}C]iodomethane were removed under vacuum, venting to a fume hood. The crude product was washed with brine (100 mL) and extracted into DCM (2 × 30 mL). The organic layer was dried over magnesium sulphate, filtered and concentrated *in vacuo*. The crude product was purified by vacuum distillation and [1′-^{13}C]1,3,5-Trimethylbenzene was obtained as a clear oil (2.95 g, 70 %).

Solution-state NMR spectra are shown in Figure S1.1. ^{1}H NMR (7.05 T, $CDCl_3$) δ (ppm): 6.96 (m, 1H C**H**), 2.43 (t+dt (2H+1H), $^{4}J_{HH}$ = 0.4 Hz, $^{1}J_{HC}$ = 126.1 Hz, C**H**$_3$). ^{13}C NMR 138.2 (d+d $^{2}J_{CC}$ = 43.9 Hz, $^{4}J_{CC}$ = 4.0 Hz, quat. **C**), 127.5 (d+d, $^{3}J_{CC}$ = 3.2 Hz, $^{5}J_{CC}$ = 0.9 Hz, **C**H), 21.7 (s, **C**H$_3$).

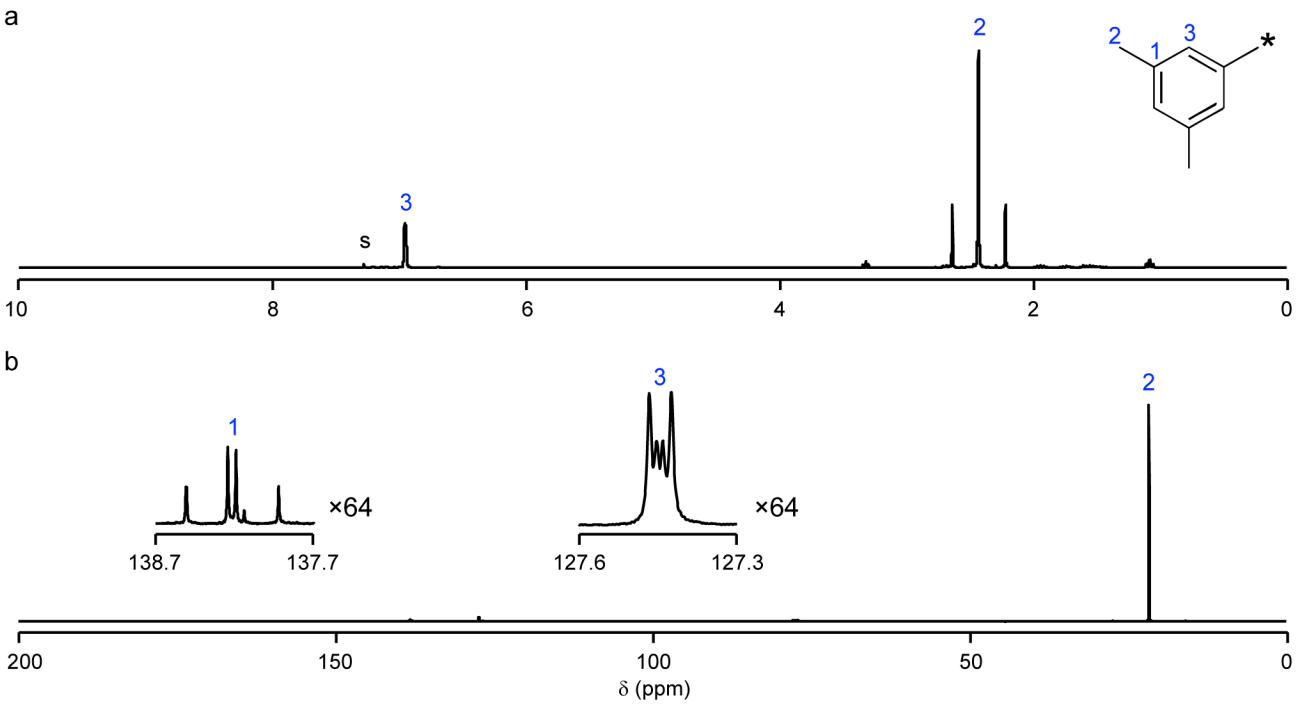

Figure S1.1: (a) ^{1}H and (b) ^{13}C NMR spectra of [1′-^{13}C]1,3,5-Trimethylbenzene (7.05 T, $CDCl_3$). The ^{1}H resonance arising from residual $CHCl_3$ in the solvent is marked s.

Benzene-1[^{13}C],3,5-tricarboxylic acid

Oxidation of the 1[^{13}C],3,5-trimethylbenzene was achieved using a modified version of the procedure of Juršić.[S1] To water (100 mL), cetyltrimethylammonium bromide (CTAB) (0.73 g; 2 mmol), [1′-^{13}C]1,3,5-Trimethylbenzene (1.25 g; 10 mmol) and potassium permanganate (14.8 g; 94 mmol) were added; the resulting suspension was then stirred vigorously and heated between 90 and 100 °C. After 6 hours the suspension was cooled to room temperature and the reaction mixture filtered through celite to remove MnO_2. The filtrate was saturated with sodium chloride and extracted with DCM (2 × 30 mL) to remove any unreacted starting material. The aqueous layer was adjusted to pH 2 by addition of 5 M hydrochloric acid. The resulting precipitate of [1′-^{13}C]Benzene-1,3,5-tricarboxylic acid) (0.96 g, 44 %) was filtered, washed with ice-cold water (3 × 10 mL) and oven-dried (110 °C).

Solution-state NMR spectra are shown in Figure S1.2. ^{1}H NMR (7.05 T, $(CD_3)_2SO$) δ (ppm): 8.6 (s+d $^{3}J_{HC}$ = 2.9 Hz ($^{4}J_{HH}$,$^{5}J_{HC}$ < 1.0 Hz) C**H**). ^{13}C NMR: 168.4 (s, **C**O_2H), 134.4 (d+d, $^{1}J_{CC}$ = 70.0, $^{3}J_{CC}$ = 3.6 Hz quat. **C**), 134.7 (s ($^{2}J_{CC}$, $^{4}J_{CC}$<1 Hz), **C**H).

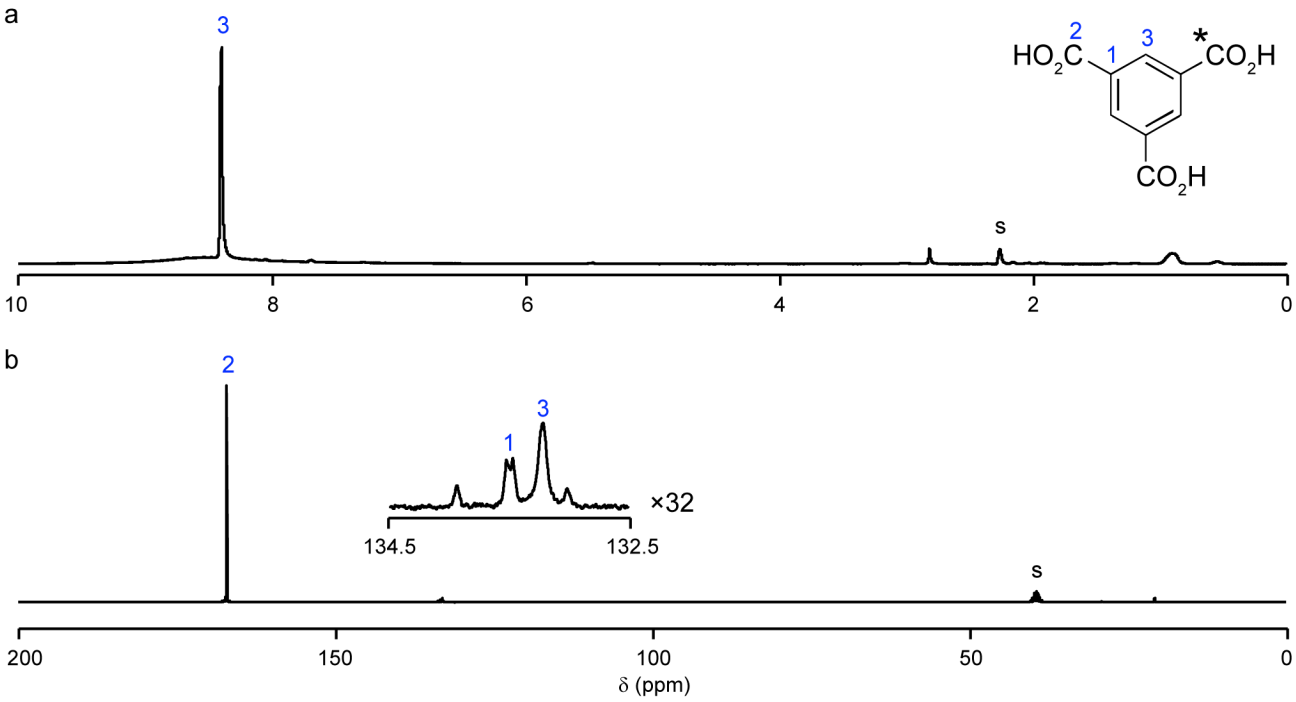

Figure S1.2: (a) ^{1}H and (b) ^{13}C NMR spectra of [1′-^{13}C]benzene-1,3,5-tricarboxylic acid (7.05 T, $(CD_3)_2SO$). The ^{13}C and residual ^{1}H resonance arising from the solvent are marked s.

1,3,5-triethyl-[U-^{13}C]benzene

$AlCl_3$ (4.77 g, 35.8 mmol) was added to a three-necked flask equipped with a reflux condenser and a dropping funnel. The condenser was fitted with a gas absorption trap containing saturated aqueous $NaHCO_3$. The flask was cooled to 0 °C and bromoethane (4.70 mL, 62.5 mmol) was added dropwise over 10 min. A mixture of benzene (2.60 mL, 29.1 mmol) and [U-^{13}C]benzene (420 µL, 4.70 mmol) was added dropwise over 15 min. The mixture was stirred at 0 °C for 20 min. Bromoethane (3.10 mL, 42.2 mmol) was added dropwise over 10 min and the mixture was warmed to RT and stirred for 12 h. The mixture was poured carefully over ice (~50 g) and the aqueous layer extracted with Et_2O (2 × 50 mL). The combined organic layers were washed with H_2O (50 mL), 1 M NaOH (50 mL), dried over $MgSO_4$, filtered and evaporated under reduced pressure. 1,3,5-Triethyl benzene and 1,3,5-triethyl $^{13}C_6$-benzene were obtained as a colourless liquid (5.35 g, 97%) and used without further purification. From the integrals of the ^{1}H NMR spectrum, some unreacted bromoethane remained. This was removed during the work-up in the next stage of the reaction sequence.

Solution-state NMR spectra are shown in Figure S1.3. ^{1}H NMR (7.05 T, $CDCl_3$) δ (ppm): 6.92 (m 1H C**H**). 2.66 (q $^2J_{HH}$ = 7.6 Hz 3H C**H**$_2$). 1.29 (q $^2J_{HH}$ = 7.6 Hz 4H C**H**$_3$). ^{13}C NMR: 144.6 (td, $^1J_{CC}$ = 57.2 Hz, $^4J_{CC}$ = 7.5 Hz) quat. **C**), 125.2 (td, $^1J_{CC}$ = 57.2, $^3J_{CC}$ = 7.5 Hz **C**H), 29.3 (s, **C**H$_2$), 16.1 (s, **C**H$_3$).

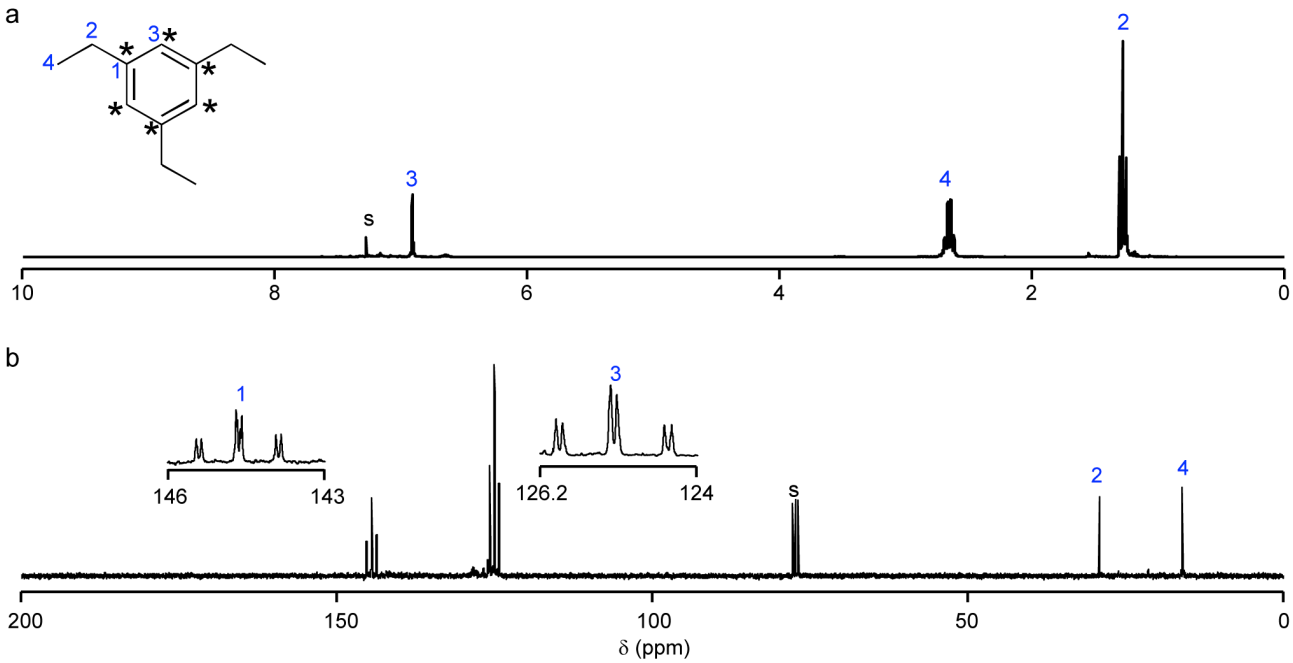

Figure S1.3: (a) ^{1}H and (b) ^{13}C NMR spectra of 1,3,5-triethyl-[$^{13}C_6$]benzene (7.05 T, $CDCl_3$). The ^{13}C and residual ^{1}H resonance arising from the solvent are marked s.

[U-^{13}C]benzene-1,3,5-tricarboxylic acid

A mixture of benzene-1,3,5-tricarboxylic acid and [$^{13}C_6$]benzene-1,3,5-tricarboxylic acid was obtained following oxidation of a mixture of 1,3,5-triethylbenzene and 1,3,5-triethyl-[U-^{13}C]benzene by aqueous $KMnO_4$ using a modified version of the procedure of Juršić.[S1] A mixture of 1,3,5-triethyl benzene (711 mg, 4.38 mmol) and 1,3,5-triethyl $^{13}C_6$-benzene (115 mg, 0.683 mmol) was added to H_2O (50 mL). CTAB (370 mg, 1.01 mmol) and potassium permanganate (8.00 g, 50.6 mmol) were added and the mixture was heated to 95 °C for 6 h. The mixture was cooled to RT, filtered on celite and the filter cake was washed with H_2O. The filtrate was acidified to pH 2 with cold 5M HCl and filtered. *n*-Butanol (10% v/v) was added and the aqueous layer was evaporated under reduced pressure. Benzene-1,3,5-tricarboxylic acid and $^{13}C_6$-benzene-1,3,5-tricarboxylic acid were obtained as a pale yellow solid (0.35 g, 32.4 %).

Solution-state NMR spectra are shown in Figure S1.4. ^{1}H NMR (7.05 T, $(CD_3)_2SO$) δ (ppm): 8.64 (s C**H**). ^{13}C NMR: 165.8 (s **C**O_2H), 125-135 (m+m **C**H and quat. **C**).

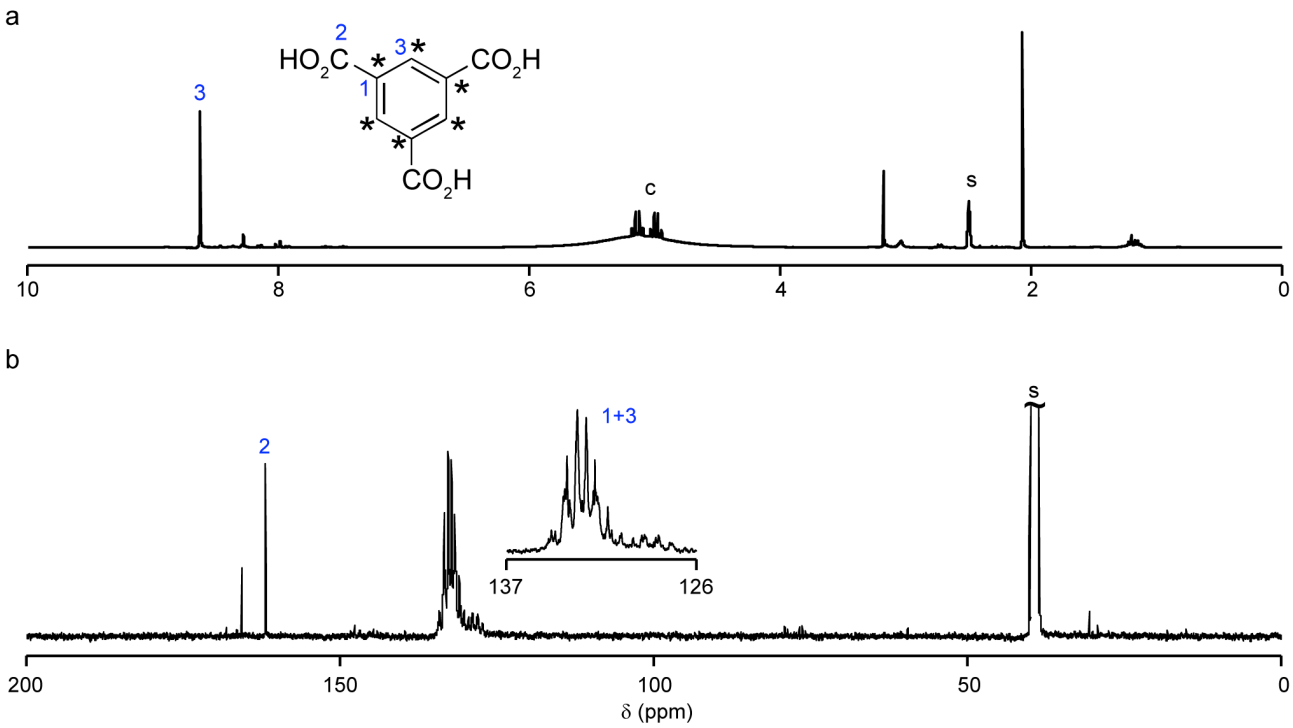

Figure S1.4: (a) ^{1}H and (b) ^{13}C NMR spectra of [$^{13}C_6$]benzene-1,3,5-tricarboxylic acid (7.05 T, $(CD_3)_2SO$). The ^{13}C and residual ^{1}H resonance arising from the solvent are marked s, and a series of resonances marked c appear to be batch-dependent contaminants in the DMSO solvent.

It should be noted that there is a relatively large shift difference for the ^{13}C resonances of benzene-1,3,5-tricarboxylic acid. This appears to be a concentration-dependent effect, as smaller masses of the labelled materials were used than for the natural-abundance material (^{13}C shifts of 166.2, 133.9 and 132.2 ppm). In addition, the CO_2**H** resonance was observed to have a very concentration-dependent shift, with values between 8.5 and 13.1 ppm observed in this work. However, the successful synthesis of both HKUST-1 and STAM-1 using benzene-1[^{13}C],3,5-tricarboxylic acid and [U-^{13}C]-benzene-1,3,5-tricarboxylic acid confirms that the above reactions produced the expected labelled benzene-1,3,5-tricarboxylic acids, despite small discrepancies in the solution-state NMR spectra.

S2. Synthesis of Cu-based MOFs

HKUST-1

The synthesis of HKUST-1 was scaled up from the previously published procedure.[S2] Copper nitrate trihydrate, $Cu(NO_3)_2.3(H_2O)$, (15.752 g, 66 mmol) and benzene-1,3,5-tricarboxylic acid (trimesic acid) (9.262 g, 44 mmol) were dissolved in an H_2O/ethanol solution (50:50) (264 ml), homogenised, sealed (600 ml autoclave) and heated at 110 °C for 1 day before being filtered and washed with H_2O and finally air-dried, yielding 15.66 g of HKUST-1.

^{13}C(2)-HKUST-1 was prepared on a smaller scale than that described above. $Cu(NO_3)_2.3(H_2O)$ (0.752 g, 3.0 mmol), trimesic acid (0.210 g, 1.0 mmol) and benzene-1[^{13}C],3,5-tricarboxylic acid (0.210 g, 1.0 mmol) were dissolved in an H_2O/ethanol solution (50:50) (20 ml) and stirred for 15 min before being sealed in a Teflon-lined steel autoclave, heated at 110 °C for 1 day, cooled to room temperature, filtered, washed with H_2O and air-dried, yielding 0.75 g of ^{13}C(2)-HKUST-1.

^{13}C(1,3)-HKUST-1 was prepared by dissolving $Cu(NO_3)_2.3(H_2O)$ (0.362 g, 1.5 mmol), trimesic acid (0.118 g, 0.6 mmol) and [U-^{13}C]benzene-1,3,5-tricarboxylic acid (0.092 g, 0.4 mmol) in 10 ml ethanol/H_2O (50:50). This solution was stirred for 15 min before being sealed in a Teflon-lined steel autoclave, heated at 110 °C for 1 day, cooled to room temperature, filtered, washed with H_2O and air-dried, yielding 0.62 g of ^{13}C(1,3)-HKUST-1.

STAM-1

The synthesis of STAM-1 followed the published procedure.[S3] $Cu(NO_3)_2.3(H_2O)$ (0.991 g, 4.1 mmol) and trimesic acid (0.862 g, 4.1 mmol) were mixed with 20 ml of MeOH/H_2O (50:50) in a Teflon-lined steel autoclave. The mixture was stirred for 15 min at ambient temperature before heating at 110 °C for 7 days. The autoclave was cooled to room temperature, and large blue crystals were isolated by suction filtration and dried in air. CD_3-STAM-1 was prepared as above, but with CD_3OD in place of CH_3OH.

^{13}C(2,6)-STAM-1 was prepared by a modified version of the above procedure. $Cu(NO_3)_2{\cdot}3(H_2O)$ (0.496 g, 2.0 mmol), trimesic acid (0.215 g, 1.0 mmol) and benzene-1[^{13}C],3,5-tricarboxylic acid (0.215 g, 1.0 mmol) was mixed with 10 ml of MeOH/H_2O (50:50) in a Teflon-lined steel autoclave. The mixture was stirred for 15 min at ambient temperature before heating at 110 °C for 5 days. The autoclave was cooled to room temperature, and blue crystals of ^{13}C(2,6)-STAM-1 were isolated by Buchner filtration and dried in air, yielding 0.59 g of ^{13}C(2,6)-STAM-1.

^{13}C(1,3,4,5)-STAM-1 was prepared by dissolving $Cu(NO_3)_2{\cdot}3(H_2O)$ (0.496 g, 2.1 mmol), trimesic acid (0.243 g, 1.2 mmol) and [U-^{13}C]benzene-1,3,5-tricarboxylic acid (0.188 g, 0.9 mmol) in 10 ml MeOH/H_2O (50:50) in a Teflon-lined steel autoclave. The mixture was stirred for 15 min at ambient temperature before heating at 110 °C for 6 days. The autoclave was cooled to room temperature, and blue crystals of ^{13}C(1,3,4,5)-STAM-1 were isolated by Buchner filtration and dried in air, yielding 0.49 g ^{13}C(1,3,4,5)-STAM-1.

S3. Packing of moisture-sensitive samples into NMR rotors

For dehydrated samples, a freshly-prepared sample was used each time a rotor was packed. Packing of samples was initially carried out under flowing argon, but samples packed rapidly in ambient conditions did not hydrate appreciably during packing. Hydration of samples was not observed once packed into rotors but, upon unpacking, the dark blue samples were observed to turn bright blue very rapidly. Figure S3.1 demonstrates that a sample of dehydrated -HKUST-1 (deh-HKUST-1) was packed under air, and rotated for 1.5 h without appreciable hydration. Therefore, all samples described in the text as dehydrated can be assumed to remain dry for the duration of the NMR experiments.

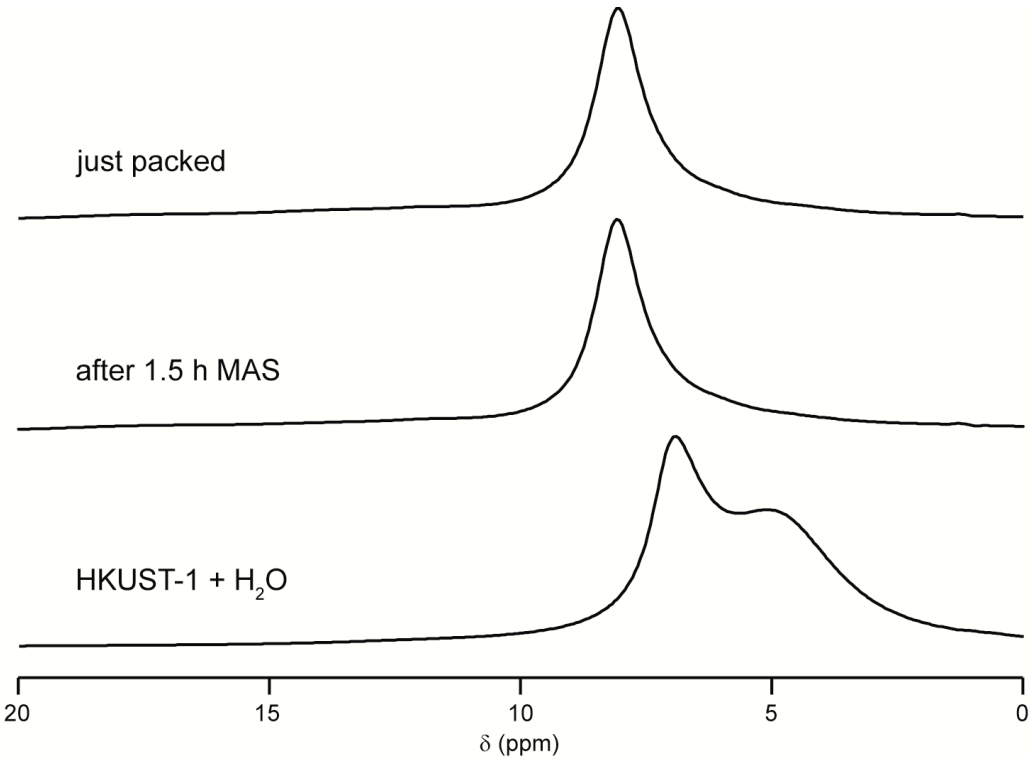

Figure S3.1 ^{1}H (14.1 T, 60 kHz MAS) NMR spectra of deh-HKUST-1 packed under air immediately after packing (top) and after being subjected to MAS for 1.5 h (middle). For comparison, the ^{1}H MAS NMR spectrum of fully-hydrated HKUST-1 acquired under the same conditions is shown (bottom). All observed chemical shifts agree with those published in Ref. [S4].

S4. Inversion recovery measurement of T_1

T_1 relaxation constants were measured using the modified version of the inversion recovery experiment shown in Figure S4.1(a). The additional π pulse at the end of the sequence was included in order to refocus any broad resonances, and τ was always one rotor period (16.67 μs). The recovery duration, τ_{rec}, was varied as appropriate to the peak(s) under consideration and pulses were always applied as close as possible to on-resonance for each peak, in order to ensure complete inversion in all cases. The dataset shown in Figure S4.1(b), for the resonance at δ = 850 ppm, in HKUST-1 shows the typical level of noise in the spectra. Using the built-in relaxation analysis module in Topspin 2.1, data were fitted to the function $I_{\tau_{rec}} = I_0(1 - 2Ae^{-\tau_{rec}/T_1})$, where A and I_0 are fitted constants with ideal values of 1, and $I(\tau_{rec})$ is the magnetisation recovered after the duration, τ_{rec}. A typical fit is shown in Figure S4.1(c), with error bars calculated by $\Delta I = N \times n$, where N is the number of data points considered as "signal" and n is the mean absolute noise per point in a region of the spectrum containing no signal (here, the region between 1000 and 1500 ppm was chosen).

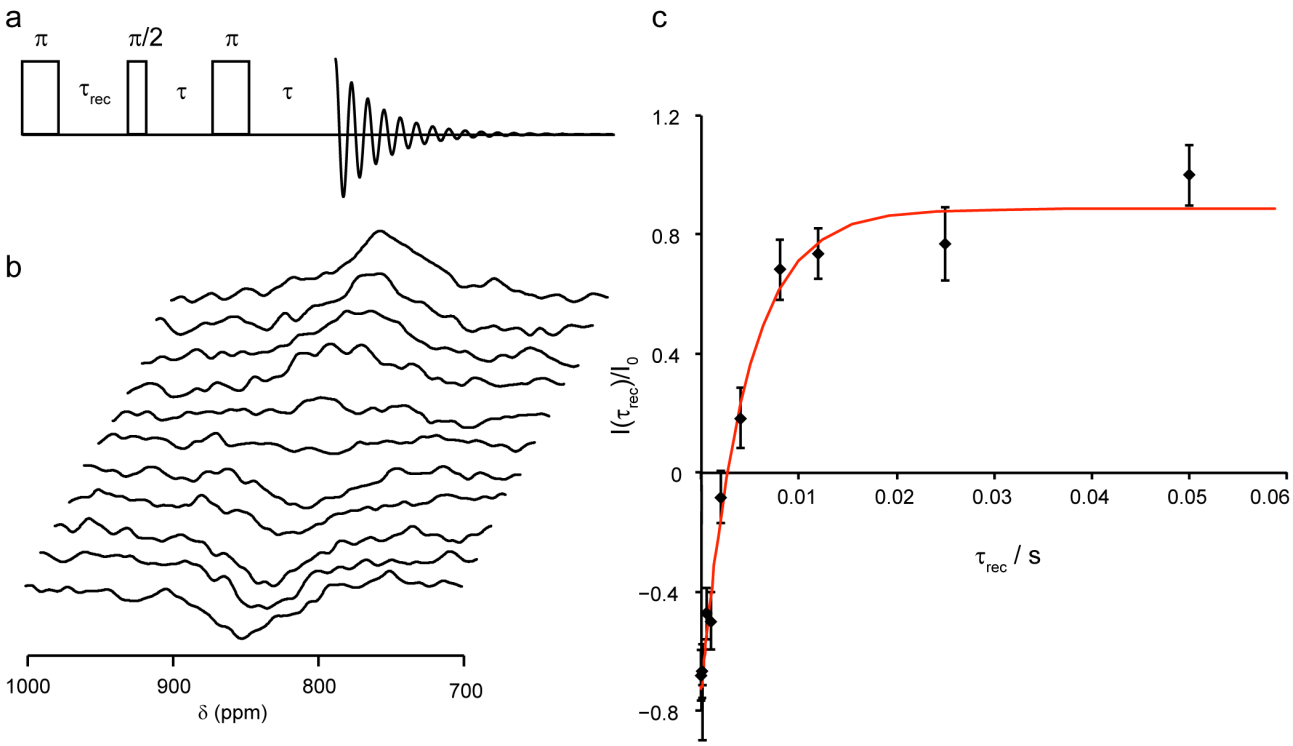

Figure S4.1 (a) Pulse sequence used in inversion recovery measurements. Flip angles are indicated above pulses, τ_{rec} is the recovery duration and τ is the echo duration, set to be equal to one rotor period (16.67 μs). (b) Experimental dataset used for measuring T_1 of C1 (δ = 850 ppm) in as-made HKUST-1. Signal averaging was carried out for 81,920 transients for each value of τ_{rec}, and each row of the dataset corresponds to a point on the graph in part (c). (c) Plot of experimentally-measured $I_{\tau rec}$ against τ_{rec} (black points) and curve of best fit (red) with I_0 = 0.8868, A = 0.9098 and T_1 = 4.458 ms. The error bars were calculated as described in the text.

S5. Solution-state and solid-state NMR spectra for tmbtc and H_3btc

Diamagnetic analogues to paramagnetic compounds have previously been used to assist assignment of NMR spectra.[S5] In this work, synthesis of the diamagnetic analogues to HKUST-1 and STAM-1 (*i.e.*, the corresponding Zn-containing MOFs) was unsuccessful, yielding instead a phase identified as the recently-reported Zn-BTC MOF.[S6,S7] As an alternative, solution- and solid-state ^{13}C NMR spectra of the simple molecular analogues trimesic acid (for HKUST-1) and tmbtc (for STAM-1) were considered. The C environments in these MOFs can, at least to some extent, be considered analogous to those in the two molecular species considered (Scheme S5.1). The ^{13}C solution-state and CP MAS NMR spectra of these compounds are shown in Figure S5.1, and are assigned as shown. In solution, the aromatic carbons (1, 3, 4 and 5) have isotropic shifts between 125 and 140 ppm, with CH at marginally lower shift than the quaternary C in both cases. The solid-state ^{13}C CP MAS NMR spectra are further complicated by the presence of crystallographic inequivalences, leading to multiple resonances for each chemically-distinct type of carbon. The presence of four closely-spaced diamagnetic shifts precludes conclusive assignment of C1, C3, C4 and C5 in the ^{13}C MAS NMR spectra of HKUST-1 and STAM-1, as almost all combinations of assignments are supported equally well when deviation from the chemical shift in the diamagnetic compounds is the only parameter considered in assignment. However, the C7 resonance in STAM-1 (48.6 ppm) can clearly be identified by analogy to the C7 resonance in tmbtc (52.8 ppm).

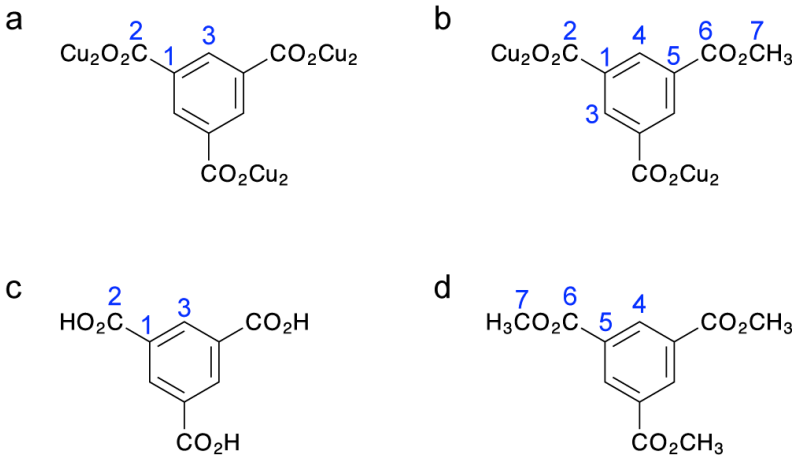

Scheme S5.1 Schematic representations of (a) btc in HKUST-1 and (b) mmbtc in STAM-1, and "model" analogues (c) H_3btc and (d) tmbtc.

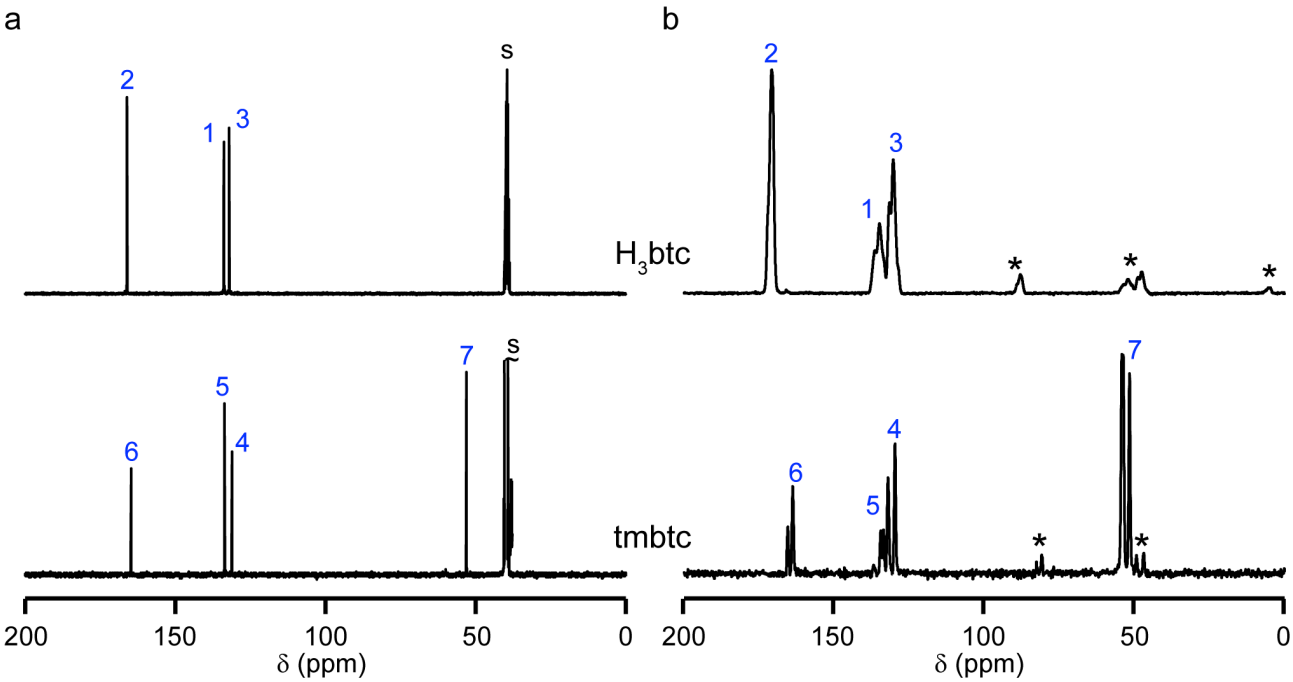

Figure S5.1 (a) Solution-state (7.05 T, $(CD_3)_2SO$) ^{13}C NMR spectra and (b) Solid-state ^{13}C (14.1 T, 12.5 kHz CP MAS) NMR spectra of H_3btc and tmbtc. Peaks marked s arise from the solvent and asterisks denote spinning sidebands.

S6. Isotropic shifts, T_1 and linewidths for ^{13}C resonances of as-made STAM-1 (14.1 T)

Assignment of the ^{13}C NMR spectrum of STAM-1 was attempted using a combination of isotropic shift, T_1 relaxation constant and linewidth for each resonance. While this suggested clear assignments for C1, C2, C3 and C7, as discussed in the main text, it can be seen from Table S6.1 that all three of these parameters are too similar to distinguish between the resonances known to result from C4, C5 and C6.

Table S6.1 ^{13}C isotropic shifts (δ_{iso}), T_1 relaxation constants and linewidths for the resonances identified as C4, C5 and C6 in as-made STAM-1

δ_{iso} (ppm)	T_1 / ms	linewidth[a] / Hz
181 (1)	7.5 (10)	465 (50)
178 (1)	15.1 (10)	420 (50)
174 (1)	13.7 (10)	290 (30)

[a]Linewidths were measured using the DMFit software.[S8] The error margins indicate the change in linewidth depending on the relative degree of Gaussian and Lorentzian character of the peaks used in the decomposition.

S7. ^{1}H NMR of CD_3-STAM-1

CD_3-STAM-1 was synthesised using a 1:1 CD_3OD : H_2O solvent in order to investigate the mechanism of monoesterification in STAM-1. As shown in Figure S7.1(a), the ^{1}H MAS NMR spectrum of STAM-1 contains a resonance corresponding to H7 at –0.6 ppm, which is absent in the ^{1}H MAS NMR spectrum of CD_3-STAM-1. However, the ^{13}C MAS NMR spectra (Figure S7.1(b)) confirm that the sample was, indeed, STAM-1 in both cases. As discussed in greater detail in the main text, the ^{13}C resonance resulting from C7 was present in the CP MAS NMR spectrum of STAM-1 when a short (250 μs) contact time was used, whereas no such resonance is present for CD_3-STAM-1 under the same experimental conditions. The ^{1}H and ^{13}C MAS and ^{13}C CP MAS spectra for these two samples confirm the assignment of the ^{1}H resonance at –0.6 ppm as H7 and the ^{13}C resonance at 49 ppm as C7.

The synthesis of CD_3-STAM-1 also provides insight into the mechanism of formation of mmbtc in STAM-1, which has previously been proposed to involve *in situ* Cu-catalysed methylation of the btc by methanol, and its subsequent incorporation into the MOF. Indeed, it is difficult to envisage any alternative mechanism by which the CH_3 functionality could be so readily imparted to each linker molecule in the MOF. Howevrem the fact that such esterification does not occur at all in the presence of ethanol (*i.e.*, yielding HKUST-1) meant that further confirmation of the esterification mechanism was required. The use of CD_3OD in place of CH_3OH in the synthesis of STAM-1 results in incorporation of CD_3 into the ester group of the mmbtc linker, confirming the mechanism previously proposed for the formation of mmbtc in the STAM-1 synthesis, although the role of Cu^{2+} in catalysing the esterification process cannot be confirmed by this experiment alone.

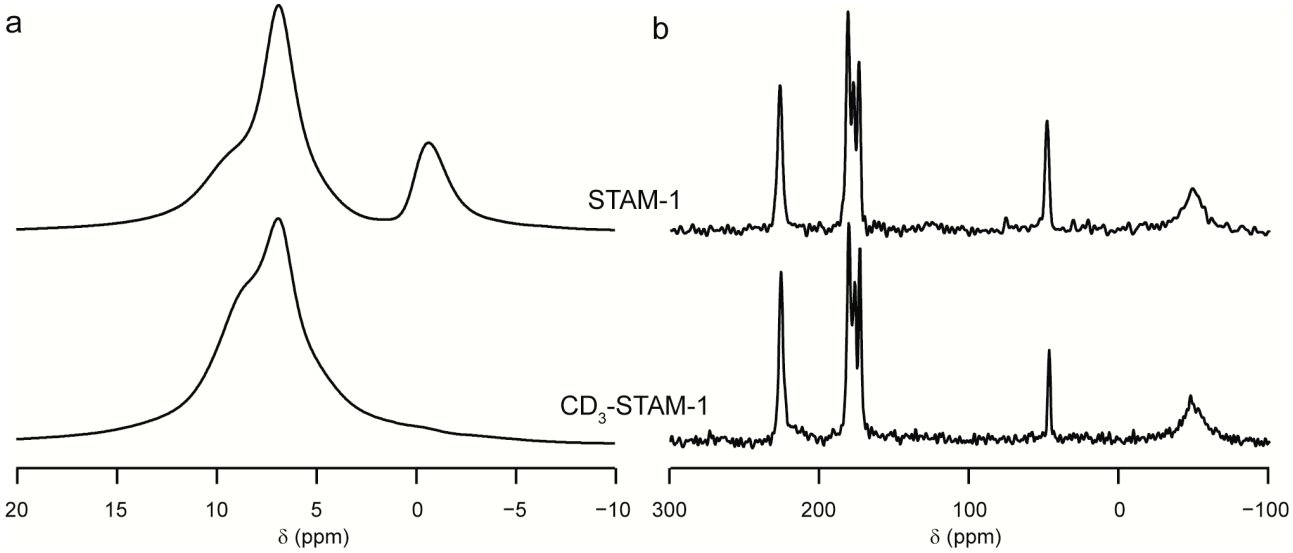

Figure S7.1 (a) ^{1}H and (b) ^{13}C (14.1 T, 60 kHz MAS) NMR spectra of STAM-1 and CD_3-STAM-1. Spectra were acquired with signal averaging of 512 transients (^{1}H) or 131,072 transients (^{13}C) using recycle intervals of 20 or 100 ms, respectively.

S8. XRD of isotopically-enriched ^{13}C(1,3,4,5)-STAM-1

The powder X-ray diffraction (XRD) pattern of ^{13}C(1,3,4,5)-STAM-1 is shown in Figure S8.1. By comparison to the simulated patterns for STAM-1 and HKUST-1, also shown in Figure S8.1, it can be seen that the majority of the sample consists of STAM-1, but some HKUST-1 is clearly present. This is not surprising, as HKUST-1 is known to be present as a low-level of impurity in many syntheses of STAM-1.[S9] From the relative intensities of the resonances at 227 ppm and 181 ppm, the molar ratio of HKUST-1 to STAM-1 in the sample was estimated to be 1 : 8. This value is based on the assumption that the resonance at 227 ppm corresponds only to C3 in ^{13}C(1,3,4,5)-STAM-1 and C3 in ^{13}C(1,3)-HKUST-1, the resonance at 181 ppm arises only from C4 in ^{13}C(1,3,4,5)-STAM-1 and the labelled linkers are distributed uniformly through both MOFs.

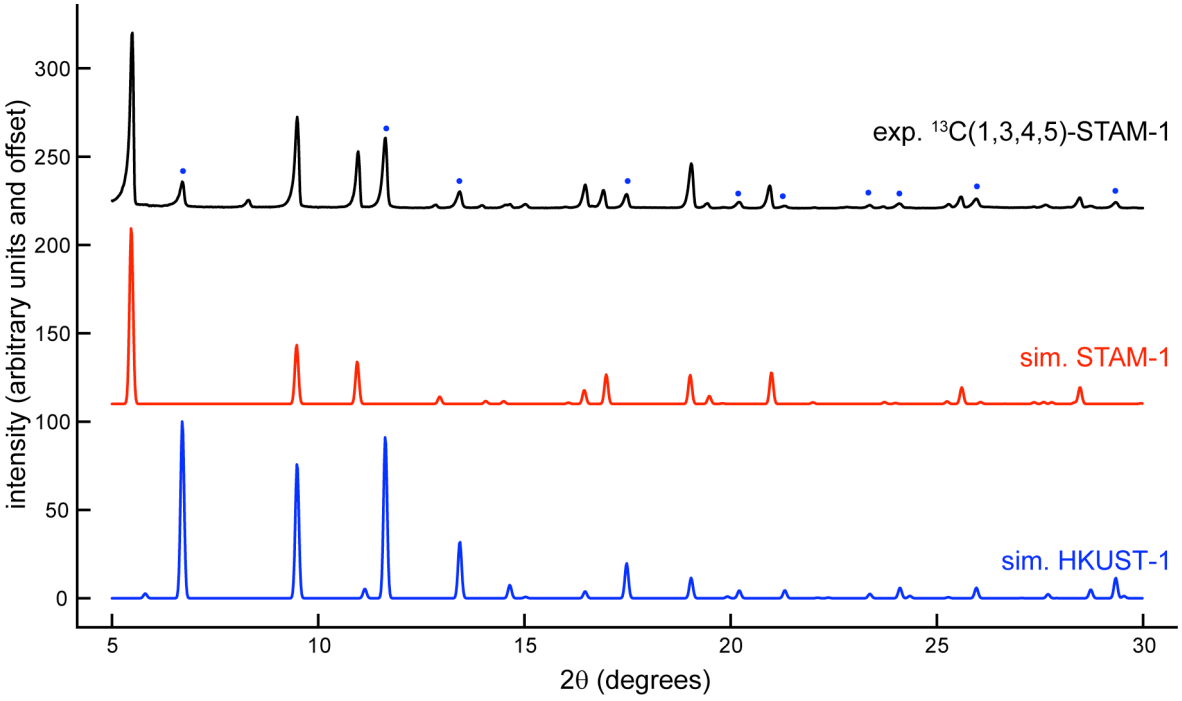

Figure S8.1 (a) Experimental powder XRD pattern of ^{13}C(1,3,4,5)-STAM-1 and simulated patterns for (b) STAM-1 and (c) HKUST-1. Peaks in the experimental diffraction pattern arising exclusively from HKUST-1 are marked in blue. The XRD pattern was obtained on a Stoe STADIP EMPYREAN diffractometer, using Cu $K_{\alpha 1}$ radiation (λ = 1.5406 Å).

S9. Extraction of isotopically-enriched mmbtc

As demonstrated by Mohideen *et al.*, STAM-1 is an excellent "protecting group" in the selective monomethylation of btc; a potentially important synthetic procedure. The methylation and "protection" steps of the reaction occur simultaneously and with high yield, and the "deprotection" step is simply a case of hydrolysis of the MOF with NaOH.[S3] When the MOF is STAM-1, careful hydrolysis with NaOH yields exclusively Na_2mmbtc (Figure S9.1(a) and Figure S9.2(a)). However, as shown in Sections S8 (above) and S10 (below), both ^{13}C(2,6)-STAM-1 and ^{13}C(1,3,4,5)-STAM-1 contained a mixture of HKUST-1 and STAM-1, and so it is no surprise that some Na_3btc was obtained upon hydrolysis of these samples, as demonstrated by ^{1}H and ^{13}C NMR spectra (Figures S9.1(b and c) and S9.2(b and c)). However, the extraction of the labelled Na_2mmbtc from both samples confirmed that the labelled linkers had been successfully incorporated in the MOFs. These results demonstrate that, while the initial cost of labelling may be relatively high, the labelled compounds can be recovered from the MOFs after use and, potentially, recycled, reducing the cost of the labelling process. In addition, the mmbtc moiety has been proposed as a core for dendrimer synthesis, and the ability to selectively ^{13}C-label Na_2mmbtc may prove to be of great use in the field of dendrimer chemistry.

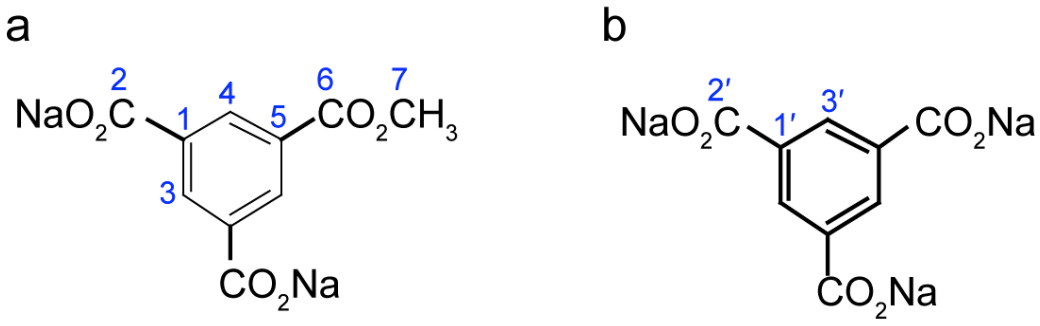

Scheme S9.1 Structures of Na_2mmbtc and Na_3btc. The numbering scheme used to assign ^{1}H and ^{13}C NMR spectra is given in blue.

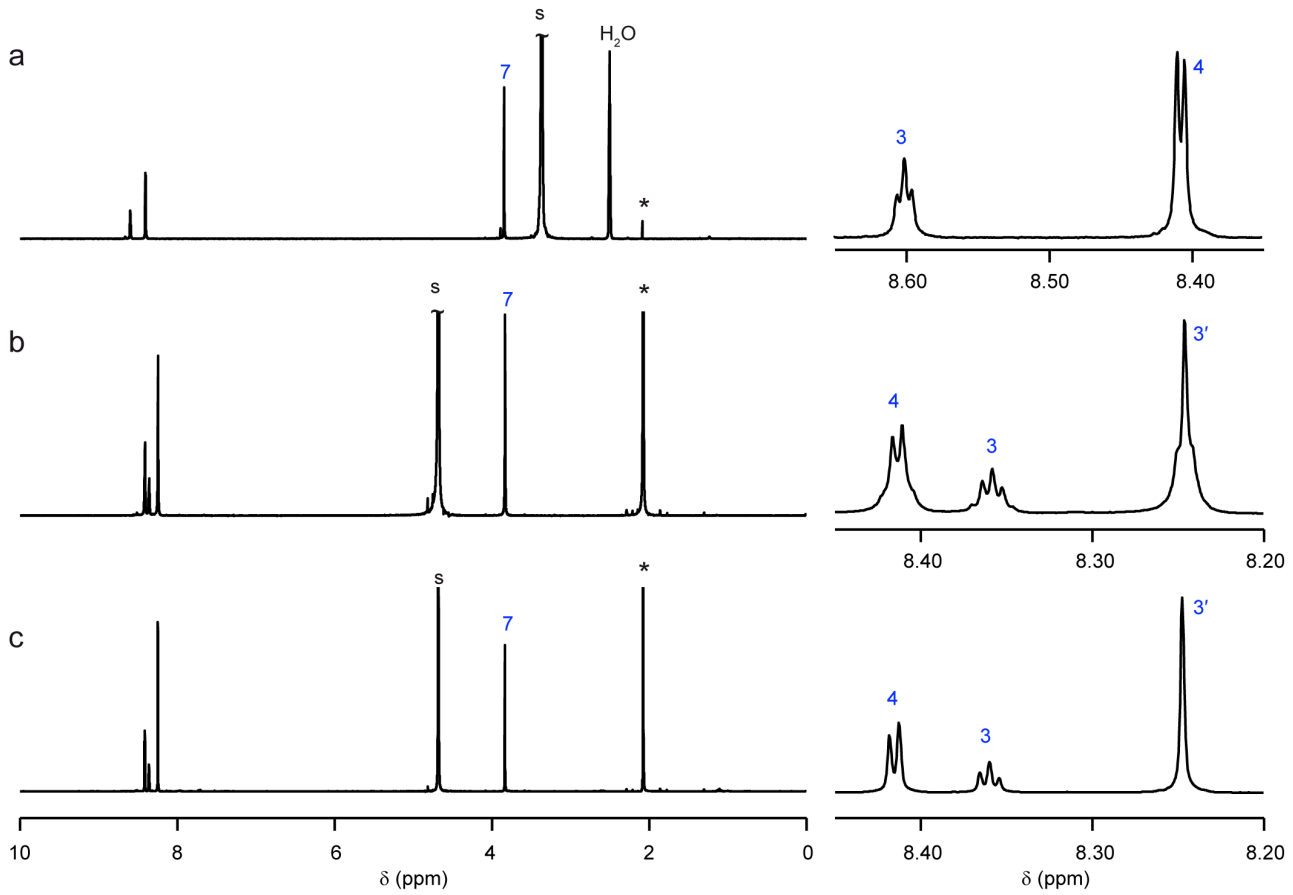

Figure S9.1 Solution-state (7.05 T) ^{1}H NMR spectra of (a) Na_2mmbtc extracted from natural-abundance STAM-1 (solvent = $(CD_3)_2SO$), (b) a mixture of Na_2mmbtc and Na_3btc extracted from ^{13}C(2,6)-STAM-1 (solvent = D_2O) and (c) a mixture of Na_2mmbtc and Na_3btc extracted from ^{13}C(1,3,4,5)-STAM-1 (solvent = D_2O). Spectra are assigned according to Scheme S9.1. Resonances marked s arise from the solvent and asterisks denote resonances arising from trace acetone.

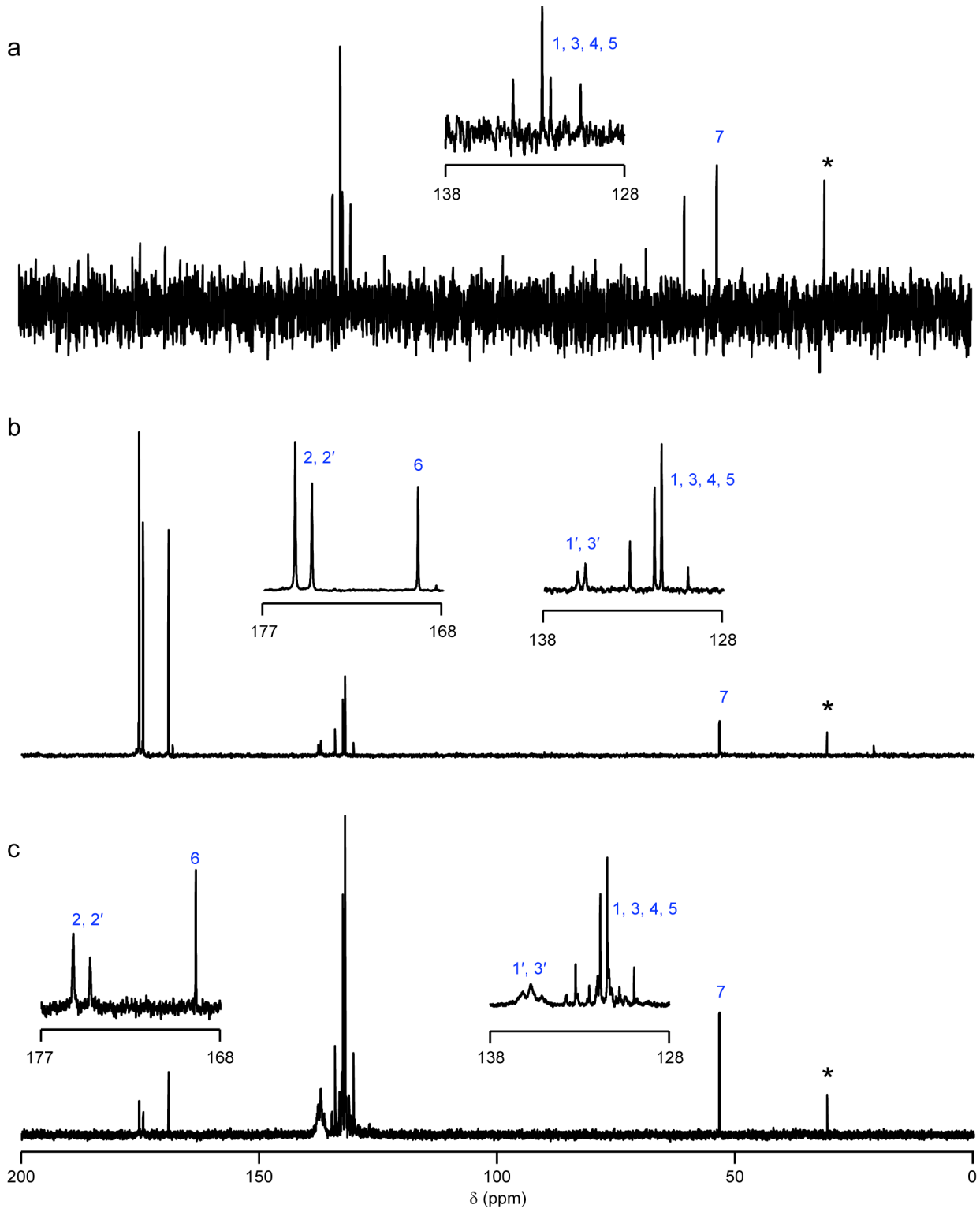

Figure S9.2 Solution-state (7.50 T, D_2O) ^{13}C NMR spectra of (a) Na_2mmbtc extracted from natural-abundance STAM-1 (solvent = $(CD_3)_2SO$), (b) a mixture of Na_2mmbtc and Na_3btc extracted from $^{13}C(2,6)$-STAM-1 (solvent = D_2O) and (c) a mixture of Na_2mmbtc and Na_3btc extracted from $^{13}C(1,3,4,5)$-STAM-1 (solvent = D_2O). Spectra are assigned according to Scheme S9.1. Asterisks denote resonances arising from trace acetone (used to reference the spectra, δ = 30.89 ppm[S10]).

S10. ^{13}C NMR spectra of dehydrated ^{13}C(2,6)-STAM-1

Figure S10.1 shows the ^{13}C MAS NMR spectrum of a dehydrated sample of ^{13}C(2,6)-STAM-1. It is clear from the increased relative intensities of the resonances at –54 and –88 ppm that these both correspond to crystallographically-distinct C2 sites, while the two resonances at 178 and 182 ppm correspond to crystallographically-distinct C6 sites. The change in lineshape at –88 ppm between the natural-abundance STAM-1 and ^{13}C(2,6)-STAM-1 can be explained by the presence of some dehydrated ^{13}C(2)-HKUST-1 (C2 isotropic shift of –87 ppm). This is a common impurity phase found in the synthesis of STAM-1, with the proportion varying with the exact reaction conditions used.

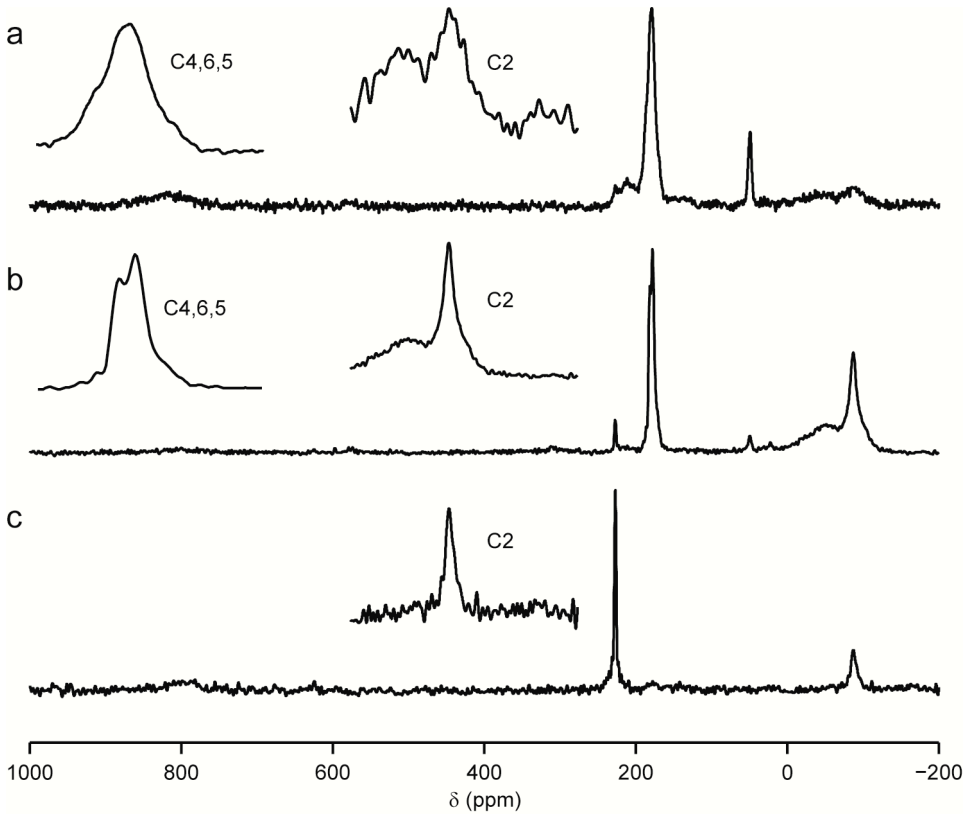

Figure S10.1 ^{13}C (14.1 T, 60 kHz MAS) NMR spectra of (a) deh-STAM-1, (b) deh-^{13}C(2,6)-STAM-1 and (c) deh-HKUST-1. Spectra were acquired in two steps with signal averaging of (a) 51200, (b) 24576 and (c) 51200 transients per step. In all cases, a recycle interval of 100 ms was used. Insets show the C2 region (0 to –200 ppm) and the C4, C5 and C6 region (200 to 150 ppm) of the spectra.

S11. ^{13}C shifts and T_1 relaxation constants at 9.4, 14.1 and 20.0 T

In order to investigate the effects of changing B_0 field strength on the observed spectra, ^{13}C spin-echo spectra were acquired for STAM-1 and HKUST-1 at 9.4 T (14 kHz MAS), 14.1 T (60 kHz MAS) and 20.0 T (58 kHz MAS). Table S11.1 present the isotropic shifts and T_1 constants measured at these three fields. Owing to the different MAS rates employed at these fields, care should be taken in comparing the data directly as the exact sample temperature is a function of MAS rate and rotor diameter. However, as discussed in the main text, the magnetic moments of HKUST-1 and STAM-1 above temperatures of ~250 K are essentially constant.[S9,S11] Therefore, the temperature dependence of δ_{iso} is expected to be negligible in the temperature regime studied here. From the field- and zero-field-cooled magnetic responses of the two MOFs, it appears that, their magnetic behaviour is field-independent as well as temperature-independent in the regimes investigated in this work.[S9,S11] The data reported in Table S11.1 appear to indicate a trend for shorter T_1 relaxation time at greater B_0 field strength (especially for C1, C2 and C3). While this observation warrants further investigation, it should be noted that the differences in measured values of T_1 are of the same order of magnitude as the margin of error on the measured values of T_1 (and, indeed, on the same order of magnitude as the smaller T_1 values). Data with reduced errors (*i.e.*, significantly increased signal to noise ratios) would be required before these observations could be confirmed. However, the prohibitively long experimental times (on the order of days to weeks per measurement) meant that such data were not acquired here.

Table S11.1 ^{13}C isotropic shifts and T_1 relaxation constants for HKUST-1 and STAM-1, measured at B_0 field strengths of 9.4, 14.1 and 20.0 T, with MAS rates of 14, 60 and 58 kHz, respectively. Measurements for C1 could not be made at 9.4 T owing to the combination of rapid T_2 relaxation and relatively long rotor-synchronised echo delay.

species	δ_{iso} (ppm)			T_1 / ms		
	9.4 T	14.1 T	20.0 T	9.4 T	14.1 T	20.0 T
HKUST-1						
C1	850 (5)	853 (5)	851 (5)	8.0 (10)	4.4 (10)	5.6 (10)
C2	–51 (2)	–50 (1)	–51 (2)	4.2 (10)	3.5 (10)	2.6 (10)
C3	228 (1)	228 (1)	228 (1)	14.3 (10)	10.8 (10)	9.5 (10)
STAM-1						
C1		853 (5)	850 (10)		3.6 (10)	2.7 (10)
C2		–50 (1)	–52 (2)	2.3 (10)	1.4 (10)	1.3 (10)
C3	228 (1)	227 (1)	227 (1)	8.9 (10)	8.5 (10)	5.9 (10)
C4	181 (1)	181 (1)	181 (1)		7.5 (10)	7.7 (10)
C5	174 (1)	174 (1)	174 (1)	15.9 (10)	13.7 (10)	18.3 (10)
C6	178 (1)	178 (1)	178 (1)	17.9 (10)	15.1 (10)	15.2 (10)
C7	49 (1)	49 (1)	49 (1)	22.4 (10)	16.2 (10)	18.4 (10)

S12. References

S1. B. Juršić, *Can. J. Chem.*, *1989*, **67**, 1381.

S2. B. Xiao, P. S. Wheatley, A. J. Fletcher, S. Fox, A. G. Rossi, I. L. Megson, S. Bordiga, L. Regli, K. M. Thomas, R. E. Morris, *J. Am. Chem. Soc.*, *2007*, **129**, 1203.

S3. M. I. H. Mohideen, B. Xiao, P. S. Wheatley, A. C. McKinlay, Y. Li, A. M. Z. Slawin, D. W. Aldous, N. F. Cessford, T. Düren, X. Zhao, R. Gill, K. M. Thomas, J. M. Griffin, S. E. Ashbrook, R. E. Morris, *Nature Chem.*, *2011*, **3**, 304.

S4. F. Gul-E-Noor, B. Jee, A. Pöppl, M. Hartmann, D. Himsl, M. Bertmer, *Phys. Chem. Chem. Phys.*, *2011*, **13**, 7783.

S5. G. Kervern, G. Pintacuda, Y. Zhang, E. Oldfield, C. Roukoss, E. Kuntz, E. Herdtweck, J.-M. Basset, S. Cadars, A. Lesage, C. Copéret, L. Emsley, *J. Am. Chem. Soc.*, *2006*, **128**, 13545.

S6. T. Cendak, T. B. Čelič, M. Rangus, N. Z. Logar, G. Mali, V. Kaučič, presented at the 7th Alpine Conference on Solid-State NMR, Chamonix-Mont Blanc, France, 2011.

S7. T. B. Čelič, M. Mazaj, N. Guillou, V. Kaučič, N. Z. Logar, presented at the 3rd Croatian-Slovenian Symposium on Zeolites, Zagreb, Croatia, 2010.

S8. D. Massiot, F. Fayon, M. Capron, I. King, S. Le Calvé, B. Alonso, J.-O. Durand, B. Bujoli, Z. Gan, G. Hoatson, *Magn. Reson. Chem.*, *2002*, **40**, 7.

S9. M. I. H. Mohideen, Ph.D. Thesis, University of St Andrews, 2011.

S10. H. E. Gottlieb, V. Kotlyar, A. Nudelman, *J. Org. Chem.*, *1997*, 7512.

S11. X. X. Zhang, S.-Y. Chui, I. D. Williams, *J. Appl. Phys.*, *2000*, **87**, 6007.